Journal of Archaeological Science 39 (2012) 2280–2293

Contents lists available at SciVerse ScienceDirect

Journal of Archaeological Science

journal homepage: http://www.elsevier.com/locate/jas

Investigating the production provenance of iron artifacts with multivariate methods

Michael F. Charlton [a,*], Eleanor Blakelock [b], Marcos Martinón-Torres [a], Tim Young [c]

[a] UCL Institute of Archaeology, 31-34 Gordon Square, London, WC1H OPY, UK
[b] Archaeomaterials, 21 Malsis Road, Keighley, West Yorkshire, BD21 1EY, UK
[c] GeoArch, Unit 6, Western Industrial Estate, Caerphilly, CF83 1BQ, UK

ARTICLE INFO

Article history:
Received 1 November 2011
Received in revised form
19 February 2012
Accepted 25 February 2012

Keywords:
Iron
Bloomery slag
Slag inclusions
Provenance
Multivariate statistics
Experimental archaeology

ABSTRACT

The quest for suitable data, data treatments and statistical methods for identifying the provenance of iron artifacts has led to a variety of analytical strategies. Researchers working on the problem have been slow to develop or adopt the use of multivariate statistical techniques, despite their successful implementation in other archaeomaterials sourcing frameworks. This paper explores the analytical potential of a comprehensive multivariate statistical strategy for identifying the primary production origins of bloomery iron artifacts using bulk chemical analyses of bloomery smelting slag and slag inclusions in iron artifacts. This strategy includes a multivariate model for identifying distinct slag inclusion types introduced during smelting and refining. Principal component analysis and linear discriminant analysis are then applied to smelting slag training sets to create multivariate provenance fields, the chemical distributions of which are defined by kernel density estimation. Single and multi-group evaluation methods are examined. Appropriate data transformations are discussed to facilitate the projection of the chemistry of "unknown" slag inclusions into the multidimensional space generated by the smelting slag groups of known provenance. The efficacy of this strategy is demonstrated through its application to a previously examined data set derived from three iron production experiments and a published archaeological example. Results indicate that an appropriately designed multivariate strategy can be an effective tool for evaluating provenance hypotheses for bloomery iron artifacts.

1. Introduction

Iron was an important component of many preindustrial economies across Africa, Asia, Europe and North America (Rostoker and Bronson, 1990). While the identification and investigation of archaeological evidence related to the production and consumption of iron is a straightforward endeavor, evaluating models for its distribution proves more challenging. Historical documents can sometimes shed important light on the workings of the preindustrial iron economy (e.g., Childs, 1981; Smith, 1995), though data are limited, of variable quality and, in the main, restricted to the situation that existed in later medieval and post-medieval Europe. Variation in artifact form, especially so-called currency bars and other types of trade iron (Crew, 1994), provides some additional clues about distributive practices. These data in turn have given rise to several models of exchange (e.g., Cleere, 1975, 1986; Rostoker and Bronson, 1990), though none that have been empirically evaluated with archaeological data alone. A key requirement for bridging this epistemological gap is the development of some means of tracing iron objects back to their production origins.

Despite efforts to determine the provenance of iron objects since at least the mid-19th century (see Schwab et al., 2006 and references therein), little consensus has been reached on what constitutes suitable data, data treatments, and statistical methods for accomplishing this goal. Debate, too, has been limited, resulting in multiple analytical strategies and few opportunities for demonstrating their general applicability. Among the approaches taken are chemical analyses of the metal in comparison to potential ores (Devos et al., 2000), isotopic ratio analysis of the metal in comparison to potential ores (Degryse et al., 2007, 2009; Schwab et al., 2006) and, most commonly, the chemical analysis of slag inclusions (SIs) in the metal in comparison to potential ironmaking regions or ore bodies (Blakelock et al., 2009; Buchwald, 2005; Coustures et al., 2003, 2006; Desaulty et al., 2008; Desaulty et al., 2009; Gordon and van der Merwe, 1984; Hedges and Salter, 1979; Leroy, 2010, Leroy et al., 2011, 2012).

* Corresponding author. 34237 First Street, Paw Paw, MI 49079, USA. Tel.: +1 269 913 4087.
E-mail addresses: mike.charlton@ucl.ac.uk, michael.f.charlton@gmail.com (M.F. Charlton).

0305-4403/$ – see front matter © 2012 Elsevier Ltd. All rights reserved.
doi:10.1016/j.jas.2012.02.037

SIs are common to bloomery iron as well as wrought irons derived from fining or puddling processes (Gordon, 1997; Starley, 1999). Provenance applications, however, are best developed for bloomery irons (but see Dillmann and L'Héritier, 2007; Gordon, 1997; Rostoker and Dvorak, 1990; Starley, 1999 on distinguishing processes). Bloomery, or direct process, iron smelting involves the solid-state reduction of iron oxides in an ore by a carbon-based fuel and reducing agent (usually charcoal). While some of the ore's impurities are driven off as a gas or alloy with the iron, the majority must be thermochemically removed as a molten slag. The reduced particles of iron, aided by the fluid slag medium, conglomerate into an entangled mass of metal and slag called a bloom. The bloom then proceeds through several stages of secondary processing, or smithing, whereby a series of directed hammer strikes and reheats are used to expel entrapped slag and shape the metal into usable items. Some of the slag inevitably remains within the iron through all stages of refining and artifact manufacture. The chemistry of the resulting SIs, though possibly altered during the smithing process, is in principle equivalent to that of the smelting slag from which it derived as well as the chemical signatures of its ore.

All approaches to SI provenance studies contain some degree of chemical pattern matching with respect to groups of ores or slags with known provenance. Such groups are typically referred to as "training sets". The simplest methods involve comparisons between numeric compositional matrices of ores, slags and SIs (e.g., Gordon and van der Merwe, 1984). Slightly more developed graphical approaches make use of visual comparisons of linear relationships between multiple series of oxide or trace element pairs within data matrices (e.g., Coustures et al., 2003). Similar methods promote the visual comparison of oxide-ratio distributions as either univariate histograms (e.g. Buchwald and Wivel, 1998) or bivariate plots (e.g. Buchwald, 2005, 246). Blakelock et al. (2009) introduced greater statistical sophistication to oxide-ratio comparisons through the inclusion of a series of *t*-tests to evaluate the likelihood that SIs and smelting slag were derived from the same chemical population. The most complex approaches include the use of multivariate statistics as an aid for distinguishing groups (e.g., Hedges and Salter, 1979) or inferring group memberships (e.g., Leroy, 2010; Leroy et al., 2012).

This paper seeks to extend the development of multivariate data analysis in iron provenance research. Building specifically on the work carried out by Blakelock et al. (2009), a series of multivariate models are introduced for: (1) discriminating primary smelting SIs from those added or contaminated during smithing; (2) testing the provenance hypothesis of iron artifacts relative to a single production source; and (3) testing origin hypotheses of iron artifacts relative to multiple potential sources. The models are applied to the same experimental data set originally discussed in Blakelock et al. (2009) to evaluate their utility.

2. Materials and methods

2.1. Experimental design

A series of experimental iron production campaigns were hosted by the National Museum of Wales in St. Fagans between 1998 and 2004. The experiments were designed to evaluate the performance of furnace designs based on archaeological examples typical for south Wales throughout the first millennium AD and charged with ores similar to those exploited at that time. Some design features and operating parameters were also derived from insights generated by Crew's (1991) experimental program based in northwest Wales. Materials produced in three of these experiments (XP17, XP23, and XP26) were selected by Blakelock et al. (2009) for bulk chemical analysis.

XP17 utilized a low-shaft, slag-tapping furnace that was manually blown with a single accordion bellows at a variable rate. 103 kg of oak charcoal were burned at a rate that varied from 11 to 8 kg/h. The furnace was charged with 25 kg of Blaenafon siderite at a fuel to ore weight ratio of 1:1. The yield included a 2.1 kg bloom and several kilograms of tapped slag. The bloom was smithed into a bar using a small clay hearth. XP23 and XP26 shared very similar design features, being conducted in a low-shaft, slag-tapping furnace that was mechanically blown with a continuous fan blower at a rate of ≈1000 l air/min. XP23 burned 95 kg of charcoal at a rate of 15.2 kg/h and charged 25.2 kg of South African Sishen hematite at a 1:1fuel to ore weight ratio. The yield included a 6 kg bloom and several kilograms of slag, much of which was recycled into the furnace during operation. The bloom was later smithed into a billet. XP26 burned 84 kg of charcoal at a rate of 13.7 kg/h and charged 22.4 kg of Sishen hematite at a 1:1fuel to ore weight. The yield included a 4.6 kg bloom and several kilograms of slag, much of which was recycled. The bloom was later smithed into a bar. Furnace and hearth clays were obtained at the experimental site and quartz sand was used as a flux during smithing for all experiments. Chemical analyses for the raw materials used in the experiments are provided in Blakelock (2009; Table 2) and summarized again in supplemental Table S1.

2.2. Materials analysis

Blakelock et al. (2009) analyzed a wide range of materials from the experiments including smelting slag and SIs from bloom fragments (XP23, XP26), a worked bloom fragment (XP23), billets (XP23, XP26) and bars (XP17, XP26). Elemental compositions of the smelting slag and SIs were measured with an Oxford Instruments energy dispersive spectrometer attached to a Phillips XL30 scanning electron microscope (SEM-EDS) with an accelerating voltage of 20 kV and ≈100 s capture time. Oxygen was determined by stoichiometry. Accurate measurements were obtained for Al_2O_3, SiO_2, K_2O, CaO, TiO_2 and MnO concentrations, with somewhat poorer, though consistent results for MgO. Bulk compositional analyses of smelting slag specimens were made from 15 separate areas of at least 300 μm^2. Bulk compositional analyses of SIs were restricted to those with areas greater than 10 μm^2 and included between 25 and 50% of the total area with an explicit bias for larger areal proportions when possible.

2.3. Statistical analysis

The present study focuses on the analysis of slag inclusions from the final products of each experiment and the multivariate match between smelting SIs and smelting slag. Normalized chemical analyses for all experimental smelting slags and final product SIs are provided in supplemental Tables S2 and S3, respectively. All data were organized and manipulated in MS Excel and statistically analyzed in R 2.11.1 (R Development Core Team, 2010) using functions in the standard and MASS (Venables and Ripley, 2002) packages.

Measurements below detection limits for key oxides pose significant problems for multivariate analysis. First, because these values are typically replaced with zeros, they can produce artificially skewed distributions in what are otherwise continuous variables. Second, data transformations involving division or logarithms of zeros are undefined. Here, measured oxides with values below detection limits were handled in two distinct ways to allow statistical treatment. In smelting slag compositions, these measurements were replaced by the minimum non-zero recorded value for that oxide in the same experimental smelting slag set. SIs with values recorded below the detection limit in relevant oxides

were removed from further consideration. The goals of these procedures were maximization of the coverage of the training sets and minimization of erroneous SI matches to training sets.

3. Modeling smelting slag and SI chemistry

3.1. Bloomery smelting slag formation and chemistry

The production of a liquid slag is essential to bloomery smelting for several reasons including the provision of a transport medium for reduced iron particles, protection of the growing bloom from oxidation near the combustion zone of the furnace and, most importantly, the removal of non-volatile non-reducible compounds (NRCs). The most abundant non-ferrous NRC in most iron ores is silica (SiO_2), with a melting point of 1723 °C. This is significantly higher than the temperature obtained in any bloomery furnace (1100–1400 °C), necessitating silica's removal with the aid of a chemical flux. Iron (II) oxide (FeO) fulfills this role, reacting with silica to form the compound Fe_2SiO_4 that melts at around 1200 °C. Upon solidification, this forms the olivine phase fayalite, which is the dominant microstructural constituent in most bloomery smelting slags. Other common NRCs in the ore, and consequently the slag, include Al_2O_3, TiO_2, MnO, CaO and MgO.

Though the slag generally derives the bulk of its chemical composition from the ore, significant contributions are also made by dissolved technical ceramics and fuel ash (Crew, 2000). Technical ceramics are introduced as the slag attacks the inner wall of the furnace and sometimes the nose of the tuyères (e.g., Veldhuijzen and Rehren, 2007). These typically contain high concentrations of Al_2O_3 and SiO_2. The ash content of charcoal is rich in CaO and K_2O. Additional fluxes can also be added deliberately to promote greater yields of iron. These include minerals that are rich in MnO, which easily substitute FeO in the olivine mineral system, or CaO, which promotes the production of low melting temperature pyroxenes. In some cases, it may also be necessary to add SiO_2 to promote slag formation if the ore is poor in this oxide.

The final slag chemistry, expressed as a series of oxide and trace element concentrations, is a function of furnace temperature, redox conditions, reaction speed and the chemistry of the materials present in the smelt. For typical bloomery systems, these relationships are articulated by the formula (Charlton et al., 2010):

$$C_{slag} = (O - R) + F + L + A - V$$

where slag chemistry (C_{slag}) is equal to the sum of all compounds and trace elements in the ore (O), less any reduced metals incorporated into the bloom, flux (F; if present), dissolved furnace lining (L) and fuel ash (A), minus any volatile compounds in the system (V). Some variation in slag chemistry is expected because of the heterogeneities associated with furnace atmospheres as well as small differences in resource compositions and operating procedures. Nonetheless, slag chemistry derived from any given smelting recipe will be distributed continuously within a single cluster when represented in multivariate space.

One implication of this model is that compositional data matrices of bloomery smelting slags obtained from single deposits and sites are appropriate units for constructing multivariate training sets. Strong anecdotal support is gathered from studies showing that slag chemical groups tend to be located in distinct clusters across space and time (e.g., Charlton, 2009; Charlton et al., 2010; Fells, 1983 Morton and Wingrove, 1972; Paynter, 2006). The success of efforts to source iron objects to such training sets rests on the degree to which: (1) variation is greater between groups than within them—the essential criteria of the Provenance Postulate (Neff, 2000); (2) biases to variability in the training set are controlled (such as the use of multiple smelting recipes or geological resources); and (3) biases to variability in SI chemistries are controlled in order to ensure they are derived from smelting slag.

3.2. SI formation and chemistry

SIs are a consequence of bloomery smelting, bloom refining and artifact production. As noted above, slag separation from the metal in the furnace is never complete and large quantities remain entangled within the bloom. Most of the slag is removed through a series of smithing operations, though numerous inclusions remain throughout all stages of refining. The smithing process, however, is not conducted in a closed system. The addition of new inclusions is possible and some alterations to the chemistry of smelting-derived SIs can occur.

Many and probably most of SIs in an object derive their chemistry directly from that of the smelting slag and they tend to maintain the same variability. Consequently, there is a strong association of SI chemistry with that of the metallic phases in which they are found (Buchwald, 2005). Where the temperature of the furnace was lowest and the redox conditions weakest, the slag tends to retain higher proportions of FeO and other reducible compounds while the iron surrounding it tends to be low in carbon. Conversely, the higher temperature/stronger redox regions of a furnace tend to produce a slag with low FeO and an iron with higher carbon. The behavior of phosphorus (measured as P_2O_5) is more complex than that of FeO, but also tends to be richer in SIs and metallic phases where furnace temperatures and CO/CO_2 ratios were relatively low. Nonetheless, the actual distribution of chemical variants in the SIs will be continuous—just like the smelting slag from which they originate.

Though smelting slag and SIs often share similar chemistries, the concentrations of reducible compounds like FeO and P_2O_5 in SIs can differ significantly in terms of their means and standard deviations. This is most likely caused by the oxidizing, but variable, atmosphere experienced by the object during smithing. The fluctuating concentrations of reducible compounds also affect the absolute concentrations of NRCs. The ratios of NRCs, nevertheless, will remain relatively constant between smelting slag and SI.

New inclusions can be introduced to an object in two main ways. First, small amounts of fuel ash and hearth clay may be inadvertently introduced to an object if hammered surfaces are not kept exceptionally clean during smithing. Second, the oxidation of iron at the object surface during smithing yields hammerscale (magnetite, Fe_3O_4) which flakes off and makes welding difficult. A common practice amongst modern experimenters is to use sand or clay fluxes that react with the magnetite to produce a liquid Fe_2SiO_4 or glassy slag, respectively. This practice makes it possible to clean the surface of existing hammerscale and prevent further oxidation. While most of the new slag will be expelled, some will inevitably remain behind to form new inclusions, especially along the weld surfaces. The frequency of new inclusions, and the potential contamination of smelting-derived SIs, increases as an object undergoes repeated processing and greater degrees of refinement (Dillmann and L'Héritier, 2007).

Finally, it is important to note that some phases can generate localized concentrations of specific NRCs in very small SIs. Dillmann and L'Héritier (2007) describe this phenomenon and illustrate its effects through analysis of SIs in an object from the Roman workshop at Les Oulches (Dieudonné-Glad, 2000). In this case, the surface area of hercynite crystals ($FeAl_2O_4$) was large relative to SI surface area and results showed abnormally high measurements of Al_2O_3 varying with SI size. This problem can in part be controlled by restricting analysis to SIs above a specific size range. Otherwise, it

should be possible to remove from consideration these and other SIs not linked directly to smelting slag via the model proposed in the next section.

4. Identifying SIs derived from smelting

Before undertaking an SI provenance analysis, it is necessary to discriminate those SIs derived from smelting slag from all others. Dillmann and L'Héritier (2007) use the linear relationship between select oxide pairs (Al_2O_3–SiO_2; K_2O–CaO; and MgO–SiO_2) implicit in the constant NRC ratio model to recognize SIs that deviate from the expected pattern. SIs that do not conform to the linear model ($r^2 \geq 0.7$) are removed from consideration in stepwise progression until a good fit is achieved. This method assumes that a statistically representative sample of SIs has been analyzed (>40 if possible) and that more uncontaminated smelting-derived SIs are present in the sample than contaminated and smithing derived SIs. When this assumption is not met, no linear pattern can be observed. This situation becomes increasingly likely as objects pass through more manufacturing stages.

While the approach taken by Dillmann and L'Héritier (2007) is logical and seems to perform well, more information might be gleaned by modeling the relationships between SI chemical groups. Table 1 summarizes some of the relationship between dominant NRCs and inclusion source, but can be expanded or contracted as necessary given the constraints of instrumentation. A series of hypotheses for identifying SI source can be deduced from this model for any sample of SIs. SI groups located at the upper extremes of strong positively correlated variables as summarized in Table 2 are hypothesized to be products of the parent material or materials whose chemistry is dominated by the same variables. This ideal model can of course be adapted to specific geologically or archaeologically supported cases where parent material chemistries follow different patterns such as the use of lateritic ores characterized by very high Al_2O_3 concentrations.

Principal Component Analysis (PCA) provides a bridge by which to visualize and explore the relationships shown in Table 1. Detailed explanations of the underlying mathematics of PCA can be found in Krzanowski (2000) though a short description will suffice for the present purposes. PCA is a multivariate method of ordination that derives a new set of uncorrelated variables from the original data matrix. Each new axis, or principal component (PC), is a linear combination of the original variables constructed such that the first PC is the line that accounts for the greatest portion of variation within the sample. The second PC accounts for the greatest portion of the remaining variation, but is constrained to be orthogonal to the first. The remaining PCs follow the same pattern, ultimately resulting in the same number of axes as the starting variables and no loss of information. However, it is typically possible to represent most of the variation present in the sample's relevant variables with only two or three PCs.

The magnitude of a variable's influence on a PC is given by its loading, a quantity between −1 and 1 that is equivalent to the correlation coefficient (r). Loadings can be graphically displayed as vectors emanating from the origin on a graph with two PCs. The cosine of the angle that obtains between any two loading vectors is equivalent to the correlation between them. The angles generated between loading vectors on the first two or three PC's provide an accurate indication of the variables' relationships in the sample and can be used effectively in graphical models. Finally, individual data points can be projected into PC space and interpreted in light of the new axes and loadings.

Table 1
Relationships between SI NRC chemistry and that of their common parent materials.

	MgO	Al_2O_3	SiO_2	K_2O	CaO	TiO_2	SrO	BaO
Bloomery slag	●	●	●	●	●	●	●	●
Clay		●	●	●		●		●
Fuel ash	●			●	●		●	
Smithing flux			●					

Table 2
Explanations for SI groups located at the upper extremes of strong positively correlated NRC pairs. LC = localized concentration effect.

	MgO	Al_2O_3	SiO_2	K_2O	CaO	TiO_2	SrO	BaO
MgO	LC/ash			ash	ash		ash	
Al_2O_3		LC/clay	clay	clay		clay		clay
SiO_2		clay	LC/flux	clay		clay		clay
K_2O	ash	clay	clay	LC/clay/ash	ash	clay	ash	clay
CaO	ash			ash	LC/ash		ash	
TiO_2		clay	clay	clay		LC/clay		clay
SrO	ash			ash	ash		LC/ash	
BaO		clay	clay	clay		clay		LC/clay

Prior to running the PCA, it is necessary to transform the raw SI chemical data in order to remove the dilution effect imparted by non-modeled compounds and to give approximately equal weight to all compounds of interest. The dilution problem can be corrected by converting the original variables to subcompositional ratios, where a subcompositional ratio is equal to the measured composition of a compound divided by the sum of all compounds of interest (Birch and Martinón-Torres, in press). Variables with large variances will dominate any PCA. In general, variables with the largest variances also tend to be those with the largest magnitudes. Most multivariate analyses of compositional data aim to consider the influence of all included variables regardless of scale. Common transformations for applying approximately equal weight to compounds of interest include (following the notation of Baxter and Freestone, 2006):

1. Standardization: $x_{ij} \leftarrow (x_{ij} - \overline{x}_j)/S_j$
2. Logged: $x_{ij} \leftarrow Log(x_{ij})$
3. Log-ratio: $x_{ij} \leftarrow Log[x_{ij}/g(X_i)]$

For the compositional matrix $\mathbf{X}$ made up of n cases and p variables, x_{ij} is the value for the jth variable of the ith case, $\overline{x}_j$ is the mean value of the jth variable, S_j is the sample standard deviation for the jth variable, and $g(\mathbf{X}_i)$ is the geometric mean of all variables in the ith composition. Note that the structure of log-ratio transformations correct dilution effects without any need for prior transformation to subcompositional ratios. Because of the similarity of results produced from log and log-ratio transformed matrices in multivariate analysis (Baxter, 2001), only the latter will be discussed.

There has been considerable debate regarding which type of transformation is appropriate to compositional data (e.g., Aitchison et al., 2002; Baxter and Freestone, 2006; Tangri and Wright, 1993). In practice, standardized and log-ratio transformations yield different but often complementary information (e.g., Neff, 1994). The analysis by Baxter and Freestone (2006) suggests that the major difference between standardization and log-ratio transformation is the emphasis placed on absolute difference in variable values and relative variance, respectively. Where absolute differences are considered important, as in the model above, standardization is a logical choice since these relationships are best preserved.

Once the data matrix has been transformed, PCA further converts it into a structure that is comparable to the model given above. Cluster analysis is then applied directly to the raw PC scores in order to objectively identify the groups present and detect outliers. The result of a hierarchical cluster analysis is plotted as

a dendrogram and the identification of clusters is made by cutting the tree at the point where the rate of agglomeration seems to drop off sharply. This requires a degree of interpretation and represents one of the weaknesses of the hierarchical clustering approach. The rationality of the final clustering solution can, however, be ascertained through its comparison with plots of PC scores (Baxter, 2006) and explanations for groups derived from patterns of oxide correlations.

In this paper, groups are identified by an average linkage cluster analysis, a type of hierarchical agglomerative algorithm that treats all cases as individual clusters and successively links them into a single cluster based on a distance or dissimilarity measure. The average linkage procedure joins clusters based on the average Euclidian distance measured between all pairs of cases in each cluster (Krzanowski, 2000). Other common clustering algorithms, such as single linkage, complete linkage and Ward's method, may reveal similar structure in PC scores of compositional data, though not with the same consistency and interpretability. Specifically, the single linkage algorithm has a known bias for "chaining" observations into elongated clusters, while both the complete linkage and Ward's method algorithms are biased toward dense spherical clusters. The exact shapes of groups within a sample of SIs from a single object are unknowable, but expected to have elliptical shapes with different sizes. The average linkage algorithm, being a compromise between the single and complete linkage methods, is appropriate for exploring SI compositional data because it performs well when empirical groups have different sizes and shapes. This observation is explored further in Section 6.

In light of the model depicted in Table 2, a PCA of relevant standardized NRCs will reveal, in combination with cluster analysis, the presence of all relevant SI groups in the sample. Groups demarked by high concentrations of positively correlated oxides related to technical ceramic (Al_2O_3, MgO, SiO_2 and TiO_2) indicate the use or accidental inclusion of clay additives during smithing. Likewise, groups characterized by high concentrations of positively correlated oxides related to fuel ash (CaO, K_2O, and MgO) indicate ash contamination during smithing. SIs derived from sand additives or whose composition is affected by localized concentration will be separated by high values along a single variable such as SiO_2 or Al_2O_3. The SI group derived from smelting slag, if present, will plot near the origin since smelting slag is a combination of multiple parent materials including clay and ash. The presence or absence of any one of these groups in a particular sample is a consequence of refining actions, skill, and analytical sampling error.

5. Multivariate models for identifying SI provenance

The basic problem of chemical sourcing is to demonstrate that the chemistry of some material sample is equivalent to the chemistry of some known parent material (the source). In the case of smelting slag and SIs derived from it, finding absolute chemical equivalence is rarely possible. As noted above, the oxidizing conditions of the smithing hearth lead to pronounced differences in FeO and P_2O_5 concentrations in the SIs relative to the smelting slag. However, NRCs in uncontaminated smelting slag and smelting-derived SIs will maintain the same ratios with each other throughout all stages of processing (Dillmann and L'Héritier, 2007). It is necessary, therefore, to model both smelting slag and smelting-derived SI chemistry in terms of NRC ratios or subcompositional ratios without considering those oxides (especially FeO and P_2O_5) and trace elements that exhibit fluctuating concentrations between production stages. The use of ratios negates the dilution biases imposed by variable amounts of FeO, P_2O_5 and similar compounds. Subcompositional ratios are favored here because they reduce the number of potential ratio variables without loss of information.

Next, the field of potential source locations must be specified. This action is performed by constructing a series of training sets based on the compositional analyses of large samples of smelting slag derived from known locations. Relevant subcompositional values are calculated for NRCs and then transformed by taking the negative of their logged values ($-\log[x_{ij}]$). The log transformation provides scale equalization without the sample-specific constraints introduced through standardization (Sayre, 1975). Because all subcompositional ratios are less than one, however, all logged values are negative. Taking the negative of the transformed values creates a positive matrix (necessary for some operations) and is equivalent to taking the log of the inverse subcompositional ratio. Some variant of log-ratio transformation as defined above should yield similar results, though this option is not explored here. The transformed compositions of the training set members are then projected into new multivariate spaces defined by PCA and Linear Discriminant Analysis (LDA). Finally, the boundaries of the training set fields are defined through Kernel Density Estimation (KDE) and become provenance hypotheses.

The basic premises behind PCA are defined above. The only difference here is the $-\log$ transformation of variables, which makes it possible to project the chemistry of samples with unknown provenance into the same multivariate space. PCA is particularly useful when comparing SI chemistry to a single accumulation of slag, but can also be effective for multiple groups. Assuming an adequately sized sample of analyses (>40; see Baxter et al., 2000) for each group, a PCA generates a coordinate system for representing the structure and extent of each smelting system's variability—their provenance fields. New data from smelting-derived SIs from artifacts with unknown provenance can then be projected into the same multidimensional space. Those SIs whose chemistries occupy a particular field are hypothetical members of that smelting system. Those SIs projected outside of a given field are rejected as possible group members.

LDA is similar to PCA in that it constructs new axes from linear combinations of the original variables, but contrasts with it in important ways (see Krzanowski, 2000). Instead of building and ordering axes according to the amount of variance explained, LDA defines and ranks axes according to the ratio of between- to within-group covariance matrices measured from predefined groups of samples. The first discriminant function is the line showing the optimal trade-off between maximizing the distances between group means and minimizing individual group variances. The second discriminant function also maximizes group mean distances relative to minimum group variance but is constrained to be orthogonal to the first discriminant function. The remaining functions follow the same pattern, ultimately generating one function fewer than the number of groups. Scores from individual group members can be projected on to the new axes, which often show greater separation between fields than is possible under PCA. Thus, the use of LDA will be explored to better separate training sets from different smelting slag groups against which "unknown" smelting-derived SIs may be compared. Scores for specimens with unknown group affiliation can also be projected into the newly constructed multidimensional space. As above, SIs that occupy a particular field become hypothetical members of that smelting system and vice versa.

Ellipsoidal confidence ellipses are routinely drawn to define provenance fields in cases where the data are assumed to be multivariate normally distributed (e.g., Glascock, 1992). When this assumption cannot be met, as is typically the case for bloomery smelting slag, empirically derived distributions such as KDEs can provide a viable, if somewhat less functional, alternative. KDEs generate a continuous frequency distribution from a sample of cases. Rather than binning cases into a series of adjacent categories

like a histogram, a KDE is created by placing a "bump" at each point and then summing the resulting heights across the axis (Baxter et al., 1997). The bumps are actually probability distribution functions with user-defined bandwidths—smoothing parameters determined in part by sample size and variance. The result is an estimation of the population density suggested by the sample. Univariate KDEs are a replacement option for smoothed histograms. Their advantages include the lack of a defined origin and a body of theory for selecting appropriate bandwidths according to sample size. Bivariate and trivariate KDEs operate in exactly the same way and are useful for highlighting point concentrations in scatter plots, revealing the structure of large data sets, and identifying groups (Baxter et al., 1997). Because bivariate KDEs are a three dimensional surface, it is possible to display them as a series of contours defined in terms of the percentage of the total point density they contain. This feature is particularly valuable for defining non-arbitrary smelting slag field boundaries for provenance analysis.

In what follows, PCA and LDA are used to generate multidimensional coordinate systems in which to represent the structure of and relationships between smelting slag training sets. The field boundaries of the training sets are defined by KDEs using the Gaussian density function. Bandwidths are selected individually for all training sets using the Sheather-Jones plug in method (Sheather and Jones, 1991), noted for its superior performance in simulations and structured empirical comparisons (Jones et al., 1996; Sheather, 2004; Venables and Ripley, 2002). Field boundaries are delineated by contours for the maximum density level containing 100% of the training set data. Smelting-derived SI scores are then projected into the relevant analytical space. For practical considerations, each object is characterized by the average of its smelting-derived SI scores and assigned group membership based on its position relative to field boundaries. When located within the boundaries of multiple fields, hypotheses for object memberships are weighted by their relative fit to individual group densities. Point densities are calculated for the location of the average object SI scores with respect to each training set. These densities are then converted to percentiles based on the proportion of training set members with lower density estimates. Objects are ultimately assigned to the group for which they have the highest percentile ranking. It is important to note that while object percentile rankings have a loose connection with probabilities of group membership, the relationships are ordinal scale in nature and the values are restricted to the particular projection of points under scrutiny.

6. Application of provenance models to products of designed experiments

6.1. Identification of SIs derived from smelting

Given the restricted scale of SEM-EDS compositional measurements, only six oxides were included in the SI identification model: MgO, Al_2O_3, SiO_2, K_2O, CaO and TiO_2. All SI data from each object were then analyzed in the manner described above. The procedure is illustrated with SI data acquired from the XP17 bar, XP23 billet and XP26 bar. A PCA was conducted on the standardized SI subcompositional data for each object and an average linkage cluster analysis carried out on their resultant scores.

The cluster analysis of the XP17 bar SI scores reveals 9 groups when the dendrogram is cut at a height of 2 (Fig. 1). Comparing group and loading structures (Fig. 2) with the SI identification model discussed above, group 4 is identified as smelting slag, groups 2, 3, 5 and 6 are derived from or contaminated with fuel ash, groups 7 and 8 are derived from or contaminated with clay and group 9 is derived from or contaminated with silica flux. Group 1 is more difficult to explain and possibly represents inclusions with both fuel ash and clay contaminants. Analyses of the XP17 bloom SIs, not shown, also revealed the presence of clay and fuel ash groups and it is likely that many of these passed into the objects smithed from it.

As noted above, most agglomerative clustering algorithms tend to produce results that are in general agreement with one another. Subtle differences, however, can affect the way groups are constructed and interpreted with respect to a given model. To illustrate these differences, cluster analyses were conducted for the XP17 bar using the single linkage, complete linkage, and Ward's method algorithms (supplemental Figs. S1–S3). The single linkage solution leads to the same inferences as the average linkage solution, though does so with a larger number of groups. The complete linkage and Ward's method solutions lead to slightly different interpretations of group structure that do not appear rational with respect to the PCA results and the SI identification model.

The cluster analysis of the XP23 billet SI scores gives five groups when the dendrogram is cut at a height of 2.5 (Fig. 3). Based on the SI identification model, the group and loading structures (Fig. 4) indicate that group 1 comprises smelting SIs, groups 4 and 5 are populated with silica flux or flux contaminated SIs and groups 2 and 3 are contaminated with clay, fuel ash or both.

Finally, the cluster analysis of XP26 bar SI scores indicates four groups when the dendrogram is cut at a height of 4 (Fig. 5). A comparison of group and loading structures (Fig. 6) with the SI identification model identifies group 1 as smelting slag, group 2 as a silica flux and fuel ash contaminated SI and groups 3 and 4 as combinations of technical ceramic and fuel ash contaminants. In this case, all non-smelting SIs are outliers and do not have a significant effect on the loading structure. This results in less secure identifications of non-smelting SI types.

Smelting-derived SIs formed the largest group in each object. The experimental objects were not subject to intensive refining as might be expected in finished items such as swords. In cases where greater processing of the metal takes place, the proportion of non-smelting SIs is expected to increase as noted above. In archaeological cases, the proportions of SI types in an object might reflect smithing skill or style. However, for investigating provenance, it is sufficient to identify the non-smelting SI and remove them from consideration prior to comparison with smelting slag training sets.

6.2. Identification of SI production origins—single group evaluations with PCA

PCAs were individually conducted on each group of experimental smelting slag to serve as training sets. Variables used are −log transformed subcompositional ratios of MgO, Al_2O_3, SiO_2, K_2O, CaO, TiO_2 and MnO. The fields occupied by each sample were then defined by contour lines containing 100% of the training set scores as generated by a KDE. Scores from smelting-derived object SIs, also in the form of −log transformed subcompositional ratios, were then projected into the multivariate space created by the smelting slag in order to hypothesize their production origins. Individual results are shown in Figs. 7–9.

With few exceptions, SI scores plot within the boundaries defined by their corresponding experimental training sets. All SI group means, however, plot within their training set boundaries. The utility of PCA as a single group evaluation tool also rests on its ability to exclude SIs derived from recipes other than that of the training set. To evaluate this, the smelting-derived XP17 bar SIs were evaluated with the XP26 training set. The results (Fig. 10) show that the XP17 bar SIs form a distinct cluster to the right of the XP26 training set field along PC01, a PC dominated by MnO. Recalling that the −log transformation causes the loadings to be

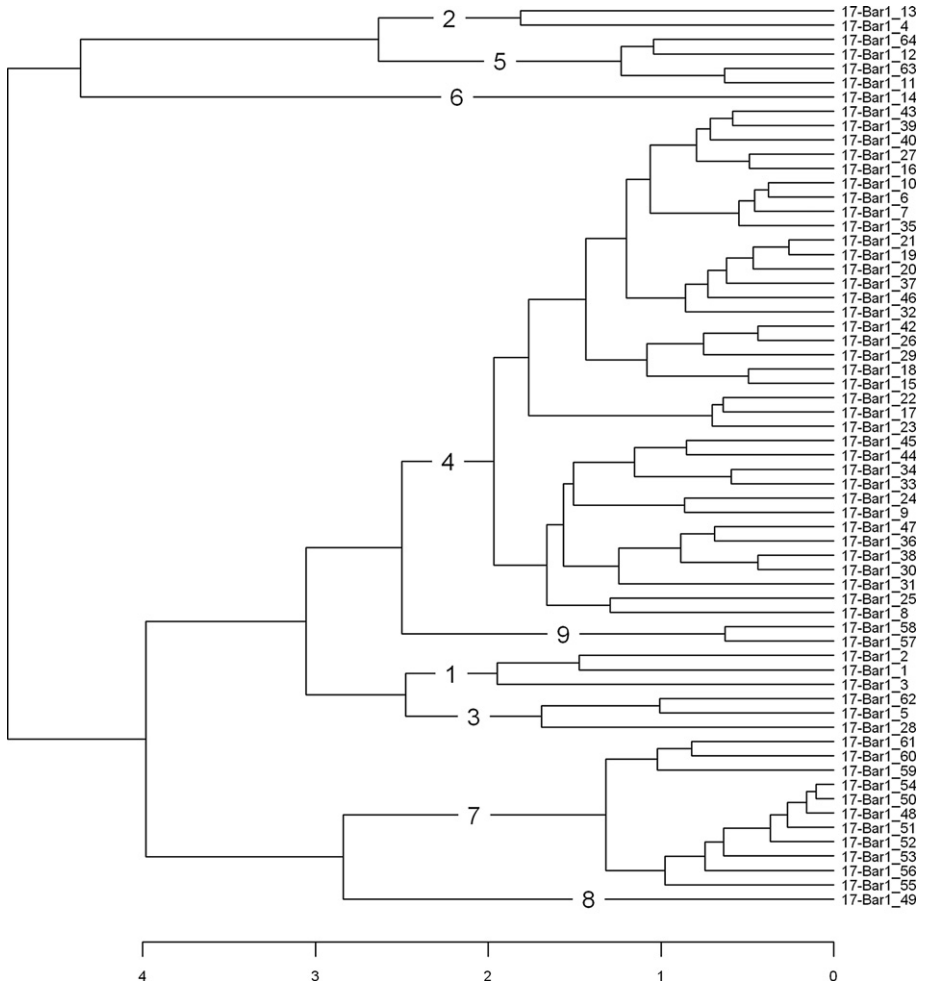

Fig. 1. Dendrogram arising from an average linkage cluster analysis of XP17 bar SI subcompositional ratios. Group identifications are indicated on cluster roots formed from cutting the dendrogram at a height of 2.

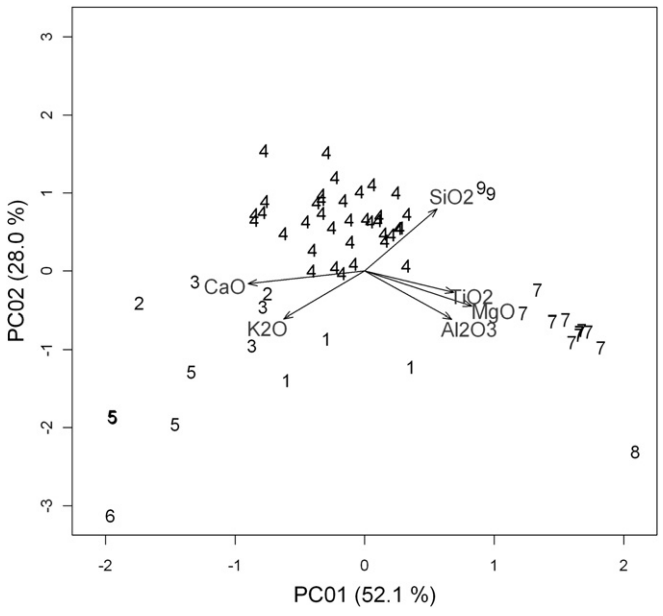

Fig. 2. XP17 bar SI subcompositional ratios projected onto the first two PC axes and labeled by group affiliation.

inverse relative to the original variables, it is apparent that the major distinction between the experimental data sets are the higher MnO contents of the XP17 slag and SIs.

6.3. Identification of SI production origins—multi-group evaluations with PCA

A PCA was conducted on the entire experimental smelting slag library using −log transformed subcompositional ratios of MgO, Al_2O_3, SiO_2, K_2O, CaO, TiO_2 and MnO. The fields occupied by each experimental subsample were then defined by contour lines containing 100% of the training set scores as generated by KDEs. As above, smelting-derived SI scores for each object were projected into the multivariate space created by the smelting slag in order to identify their production origins. Results (Fig. 11) show good separation between the XP17 training set and the others along PC01 (dominated by MnO) and subtle discrimination between XP23 and XP26 along PC02 (dominated by TiO_2 and to a lesser extent MgO). In terms of the original data, the slag and SIs derived from XP17 have higher MnO contents than those from the other experiments while the slag and SIs derived from XP26 tend to have slightly more TiO_2 and slightly less MgO than those of XP23. The poor separation between the XP23 and XP26 training sets was anticipated given the similarities in their experimental designs. All experimental smelting-derived SIs tend to cluster within the boundaries defined by their corresponding training sets, however, and the average SI

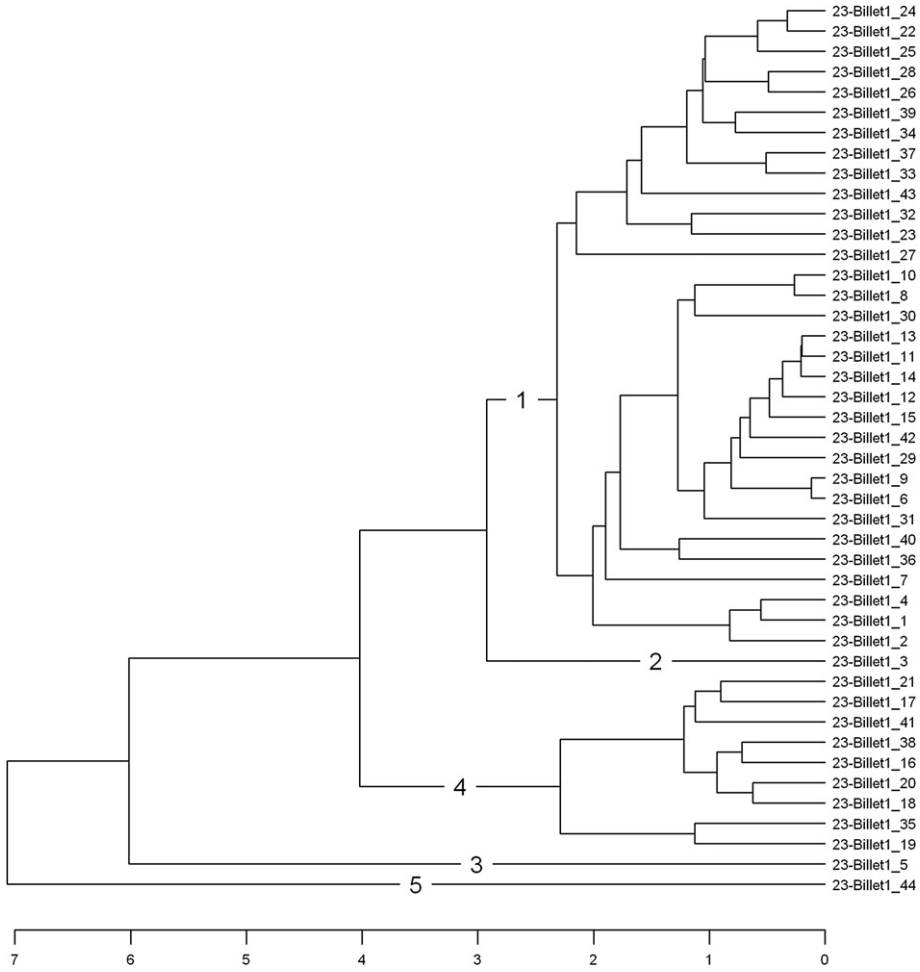

Fig. 3. Dendrogram arising from an average linkage cluster analysis of XP23 billet SI subcompositional ratios. Group identifications are indicated on cluster roots formed from cutting the dendrogram at a height of 2.5.

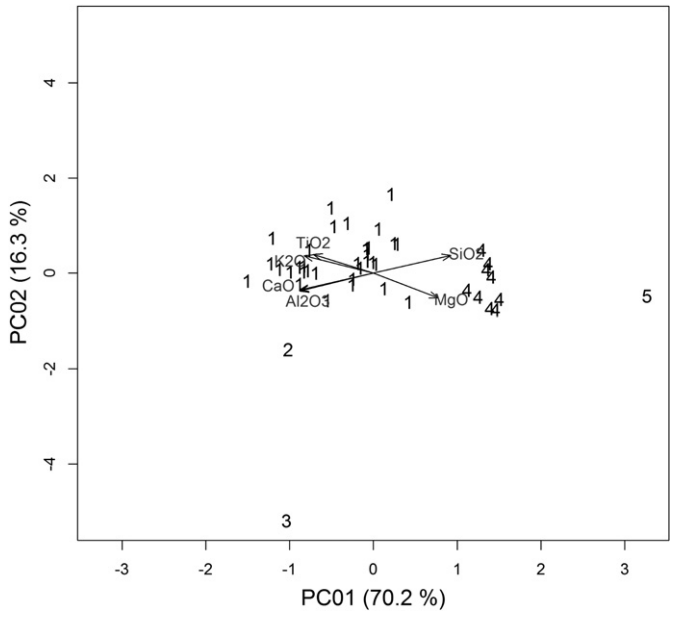

Fig. 4. XP23 billet SI subcompositional ratios projected onto the first two PC axes and labeled by group affiliation.

percentile rankings correctly identify each object to its experimental group (Table 3).

6.4. Identification of SI production origins—multi-group evaluations with LDA

A LDA was conducted on the entire experimental smelting slag library using −log transformed subcompositional ratios of MgO, Al_2O_3, SiO_2, K_2O, CaO, TiO_2 and MnO. The fields occupied by each experimental subsample were then defined by contour lines containing 100% of the training set scores as generated by KDEs. Smelting-derived SI scores were then projected into the multivariate space using the linear discriminant functions generated by the analysis of the smelting slag groups. Results (Fig. 12) show good separation between the XP17 training set and the others along LD1 (dominated by SiO_2) while subtle discrimination is apparent between XP23 and XP26 along both LD1 and LD2 (the latter also dominated by SiO_2). This partitioning is evident in the subcompositional data where slag and SIs from XP17 have the lowest mean SiO_2 content, followed by XP26 with slightly higher values and XP23 with the highest mean SiO_2 content. The separation between XP23 and XP26 is more pronounced than with PCA, but still poor. Again, all experimental smelting-derived SIs tend to cluster within the boundaries defined by their corresponding training sets and average SI percentile rankings correctly identify each object to its experimental group (Table 4).

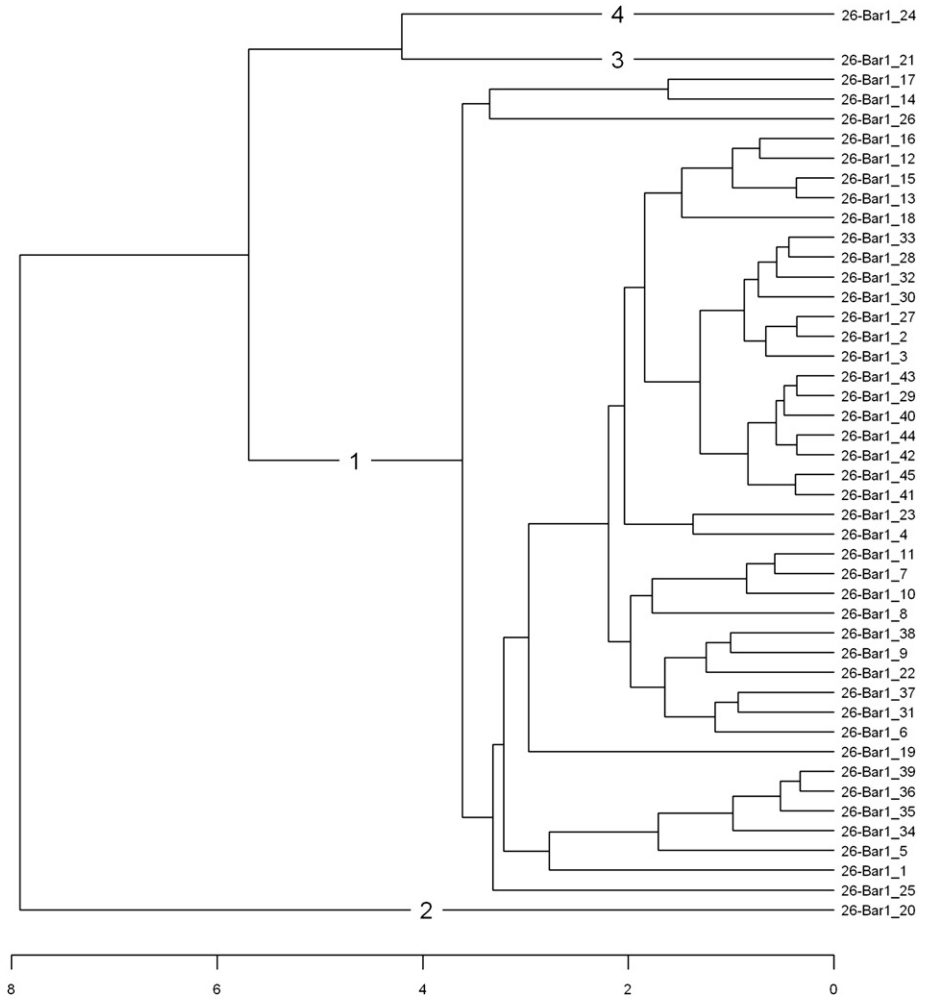

Fig. 5. Dendrogram arising from an average linkage cluster analysis of XP26 bar SI subcompositional ratios. Group identifications are indicated on cluster roots formed from cutting the dendrogram at a height of 4.

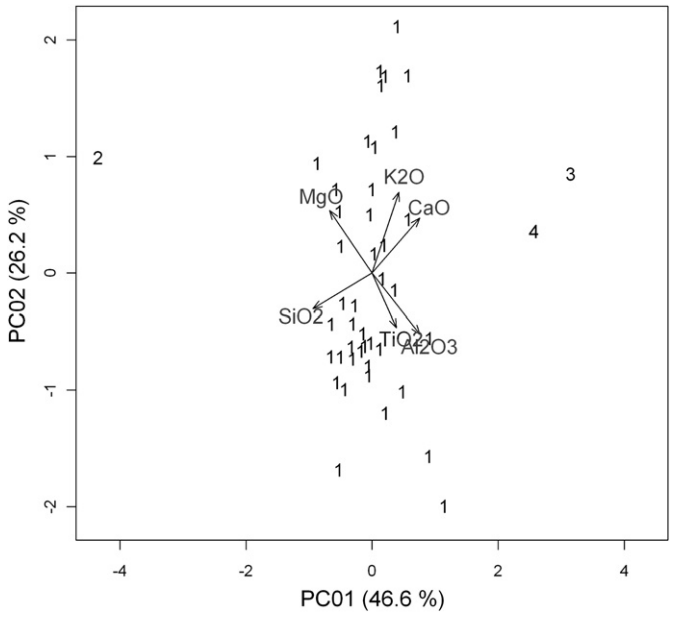

Fig. 6. XP26 bar SI subcompositional ratios projected onto the first two PC axes and labeled by group affiliation.

7. Discussion

The efficacy of the iron object sourcing strategy detailed above is clear from the results generated by its application to the products of ironmaking experiments. Indeed, the results proved better than expected by correctly discriminating the XP23 billet and XP26 bar despite the similarities of their experimental design. The strategy is, however, an ideal one implemented under controlled conditions. Whether it can withstand the rigors and complexities introduced by archaeological assemblages is a separate, but important question.

7.1. An archaeological example

At present, few archaeological smelting assemblages have been researched with the breadth necessary to sample and form adequately sized training sets at the site level. Those studies that have generated large samples tend to do so for regional levels using geographical rather than geological criteria for creating groups—a significant problem where multiple geological resources might be present. Barring this, there are also few regions, however defined, whose researchers have engaged in large scale compositional analyses of both smelting slag and SIs. Even fewer have ensured that all analyses were conducted in near identical conditions on the same instruments (or instruments for which correction factors have been calculated). This is true even of the archaeological case study presented in Blakelock et al. (2009).

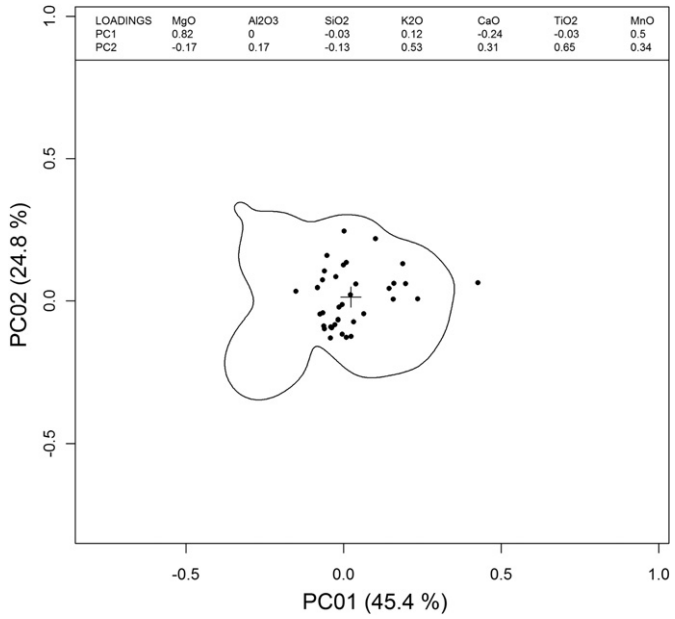

Fig. 7. Single group evaluation of XP17 production origins with PCA. Training set field defined by the KDE contour level containing 100% of the smelting slag scores. ●—XP17 bar SI scores; +—SI group mean.

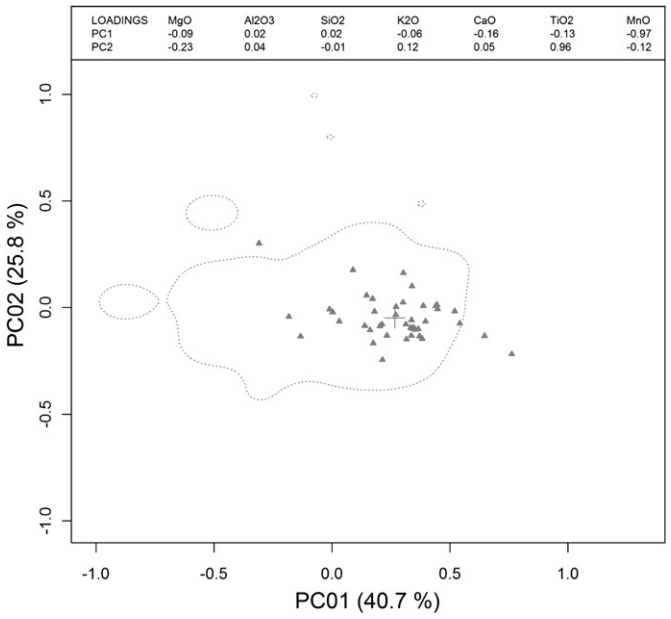

Fig. 9. Single group evaluation of XP26 production origins with PCA. Training set field defined by the KDE contour level containing 100% of the smelting slag scores. ▲—XP26 bar SI scores; +—average object SI.

The data set compiled by Vagn Buchwald (2005) for smelting slag and SIs in Scandinavia comes closest, though still falling short on key requirements. Issues relevant to the system of methods presented here include a lack of adequate sampling from object SIs (average of 2–5 analyses per metallographic zone) and insufficient sampling of smelting slag for any given site (between 1 and 10). Nonetheless, an attempt was made to adapt the system of methods presented above to the Buchwald data set. A PCA and cluster analysis of smelting slag compositions (MgO, Al_2O_3, SiO_2, K_2O, CaO, TiO_2 and MnO) showed that they form three regional groups: (1) the Danish islands Fyn and Sjaelland; (2) Western Denmark; and (3) Norway and Sweden. Using these groups of data as training sets, an LDA was conducted and previously sourced SIs projected into the multivariate space. The result is shown in Fig. 13 with points labeled according to Buchwald's provenance hypotheses based on oxide-ratio distributions (labels adjusted to match the present field names). LD1 is dominated by the influence of SiO_2 and Al_2O_3 and discriminates the Danish slag and SIs from those originating in Norway and Sweden. Indeed, Buchwald (2005) uses the SiO_2–Al_2O_3 ratio to the same effect. LD2 is dominated by SiO_2 and discriminates the training sets for western Denmark and the Danish Isles. While

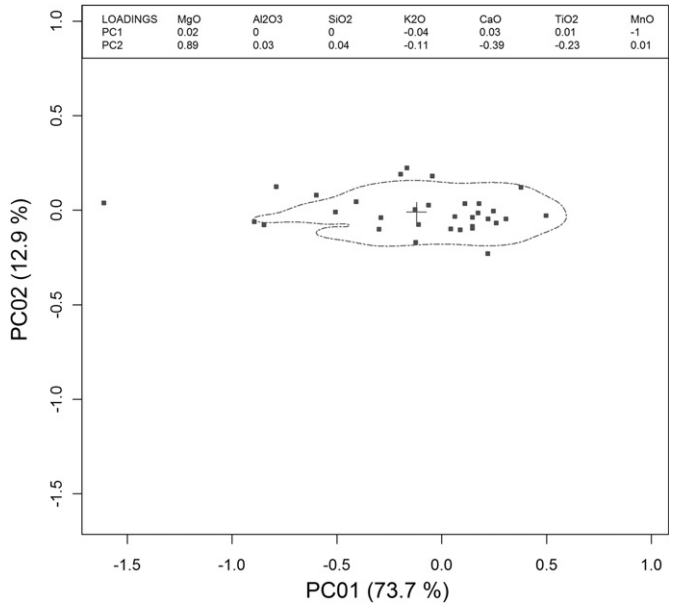

Fig. 8. Single group evaluation of XP23 production origins with PCA. Training set field defined by the KDE contour level containing 100% of the smelting slag scores. ■—XP23 billet SI scores; +—SI group mean.

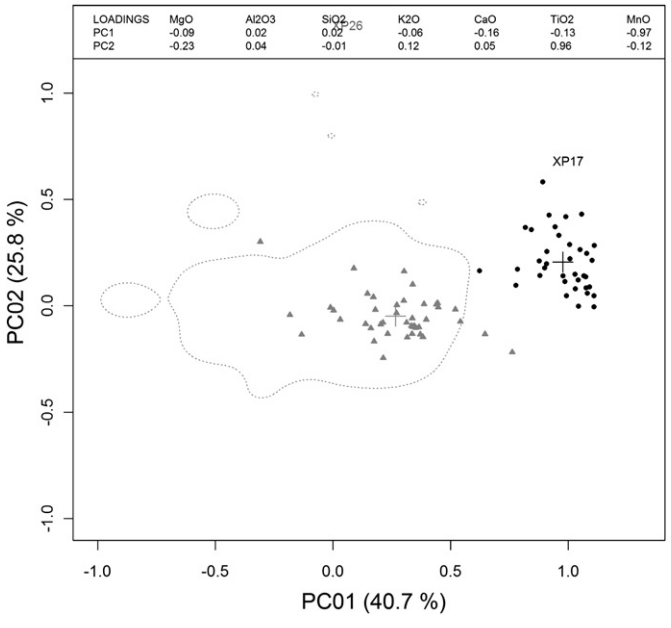

Fig. 10. Comparison of the XP17 bar SIs to the XP26 smelting slag training set. Training set field defined by the KDE contour level containing 100% of the smelting slag scores. ▲—XP26 bar SI scores; ●—XP17 bar SI scores; +—SI group means.

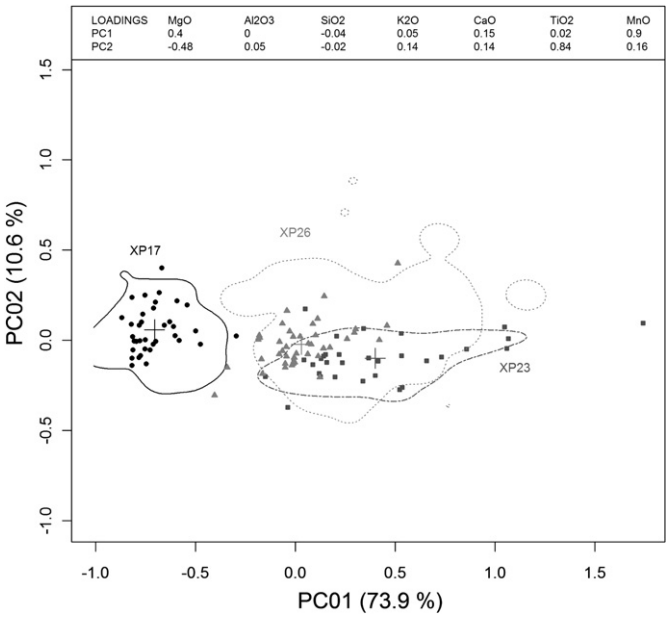

Fig. 11. Multi-group provenance evaluation using PCA. Training set fields defined by the KDE contour level containing 100% of the smelting slag scores. ●—XP17 bar SI; ■—XP23 billet SI; ▲—XP26 bar SI; +—SI group means.

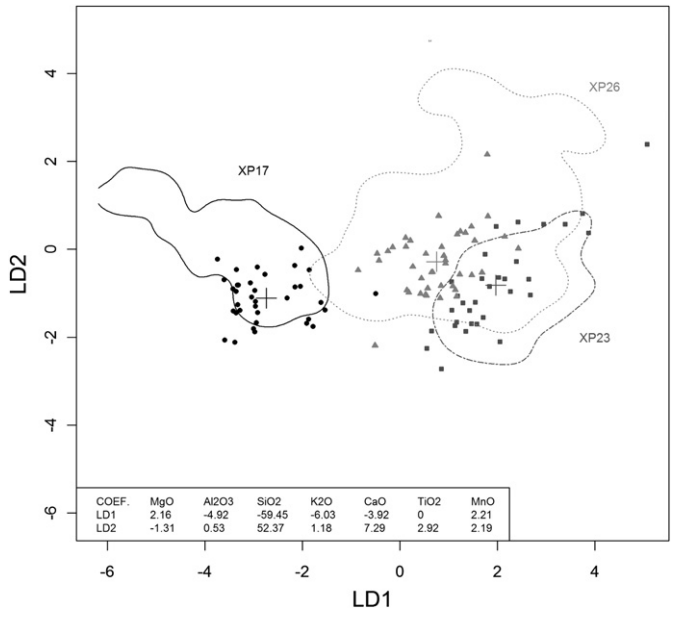

Fig. 12. Multi-group provenance evaluation using LDA. Training set fields defined by the KDE contour level containing 100% of the smelting slag scores. ●—XP17 bar SI scores; ■—XP23 billet SI scores; ▲—XP26 bar SI scores; +—SI group means.

perfect agreement been training sets and SIs could not be expected given sampling issues and the intrinsic conservativeness of the proposed methods, it is clear that the SIs plot in the "neighborhoods" of their training set fields and tend not to overlap. The two objects previously identified to Fyn-Sjaelland are an exception to this pattern and may reflect the small sample size of the training set ($n = 8$). This analysis indicates that Buchwald's identifications are reasonable and suggests that the analytical strategy developed here can be successfully deployed for archaeological cases.

7.2. Constraints to the construction and use of provenance hypotheses

The experiments and archaeological examples demonstrate the potential of the multivariate strategy described in this paper to isolate probable production sources. Production sources, however, are not determined in any absolute sense. Rather, they remain unfalsified hypotheses. In statistical terms, the analysis starts with the null hypothesis (H_0) that smelting-derived object SI chemistries are consistent with one or more of the included training sets. The region of rejection is empirically determined by KDEs. When the centroid of the smelting-derived object SIs lies outside of the KDE field boundaries, then H_0 is rejected and the alternative hypothesis (H_1)—that the chemical characterization of smelting-derived SIs in an object is not consistent with that of one or multiple slag training sets in the sampled population—is accepted. When the centroid of the smelting-derived object SIs falls within the KDE field boundaries, H_0 is not rejected. The set of H_0s that have not been rejected for any given object become origin hypotheses that might be evaluated against additional criteria. Finally, in cases where multiple provenance hypotheses have not been rejected, each is weighted according to the percentile ranking procedure. The likelihood that any unfalsified provenance hypothesis is the "true" source, however, rests on several factors including: (1) the probability that the "true" source is included amongst the training sets; (2) the degree to which discrimination between training sets can be made; and (3) the probability that the included training sets are accurate representations of their populations.

The probability that the "true" production source is present within the included training sets is impossible to determine in practice and reduces to a series of best guesses utilizing criteria such as distance, chronology, and social history. This probability will increase as slag chemistry is adequately characterized from more primary iron production sites and analytical methods become increasingly standardized between laboratories. Both situations would lead to larger numbers of training sets, but are far from reality at present.

Discrimination between training sets using major and minor oxides was demonstrated in both the experimental and archaeological examples. How well this strategy will perform in cases where larger numbers of training sets are involved is unknown. It is an unfortunate fact that the behavior of P_2O_5—an oxide useful in discriminating iron ores (e.g., Desaulty et al., 2009; Leroy et al., 2012)—prohibits its use in the SI provenance approach developed here (compare supplemental Figs. S4 and S5 to Figs. 11 and 12). Nonetheless, there are at least two ways in which this potential constraint can be mitigated. In some cases, it might prove beneficial to repeat the provenance analysis several times, removing falsified

Table 3
Percentile ranking and group assignments for experimental objects as projected into the space generated by PCA.

Object	% XP17	% XP23	% XP26	Group assignment
XP17 bar	54.82	non-member	non-member	XP17
XP23 billet	non-member	71.53	60.12	XP23
XP26 bar	non-member	5.36	84.76	XP26

Table 4
Percentile ranking and group assignments for experimental objects as projected into the space generated by LDA.

Object	% XP17	% XP23	% XP26	Group assignment
XP17 bar	79.64	non-member	non-member	XP17
XP23 billet	non-member	83.82	36.2	XP23
XP26 bar	non-member	non-member	82.26	XP26

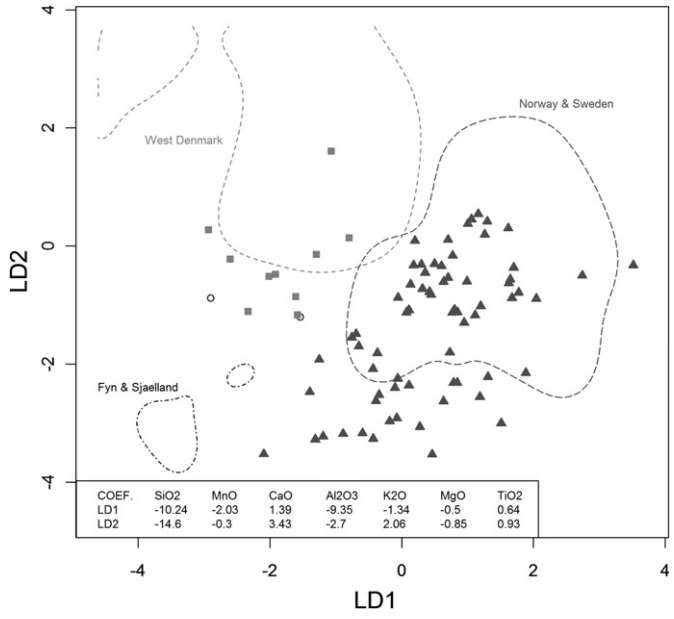

Fig. 13. Multi-group provenance evaluation of Buchwald's (2005) Scandinavian smelting slag and SI chemical library using LDA. SI symbols: ○—Fyn and Sjaelland; ■—West Denmark; ▲—Norway and Sweden. Training set data were drawn from Buchwald (2005; Tables 7.6; 8.4; 9.1; 9.3; 9.4; 9.5; 10.1; 10.5; 12.8 and 12.11). SI data were drawn from Buchwald (2005; Tables 9.1; 9.3; 9.5; 11.1; 12.1; 12.2; 12.3; 12.4; 12.5; 12.6; 12.7; 12.8 and 12.10). Data with missing or zero values were omitted from analysis.

hypotheses at each successive stage in the hope of generating better discrimination between the remaining compatible hypotheses. Another option is to extend the methods described here to additional minor and trace elements where instrumentation and costs make such a strategy feasible. Analysis of oxides and trace elements are complementary approaches to the same problem, one perhaps serving as a filter for the other.

The problem of adequate sampling of primary iron production sites is perhaps the most challenging to overcome since it requires a significant and costly change to traditional practice. Instead of analyzing a few slag specimens at a site, 40 or more will be required. Analyses conducted on training sets with insufficient sample sizes can increase the chance of committing a type I statistical error and the false rejection of a true provenance hypothesis. Indeed, this may be the case with the Fyn-Sjaelland objects in the archaeological example above.

A fourth constraint might be added to this list and concerns what is known about the particular iron object being sourced and the society that produced it. Prestige items and some military accoutrements may travel significant distances and be curated for longer periods compared to more rudimentary agricultural implements and construction materials. Similarly, a society's economy will bias the potential sources that should be included in a provenance analysis. It is probable, for example, that most of the iron objects from pre-Roman Iron Age Britain derived from local British sources given the scale of the economy and Strabo's inclusion of iron as one of the island's chief exports (Hamilton and Falconer, 1903). By the Middle Ages, however, Britain imported substantial quantities of iron from Spain (Childs, 1981; Salzman, 1952), much of which seems to have been used in construction projects (Threlfall-Holmes, 1999).

The complexities of provenance analysis are not limited to the strategy used here, but are endemic to all attempts to source iron and other materials. Nonetheless, programs of focused research can still shed light on the distribution of iron objects in the archaeological record as demonstrated by Buchwald (2005). The challenge faced by researchers is to develop questions that can be addressed adequately within the known constraints while also making strides to overcome present limitations with the construction of larger databases and greater inter-laboratory cooperation.

7.3. Applying the multivariate strategy in future work

There are three recommendations for applying this analytical strategy in future studies. First, the structure of the smelting slag training sets should be characterized in order to identify the potential presence of multiple groups and any significant outliers. Such operations will be essential in archaeological cases to avoid biases due to measurement errors, inclusion of corroded samples, and the incorporation of multiple smelting recipes. Second, the SI identification model can be further refined to decrease the inclusion of contaminated specimens. The procedure, following Baxter (2006), involves conducting a secondary *k*-means cluster analysis using the number of clusters and initial cluster centroids derived from the results of the initial average linkage cluster analysis. A drawback to *k*-means clustering is the method's tendency to artificially divide elliptical clusters into two roughly equally sized groups—the reason it was not applied in this study. However, it is sensitive to extreme outliers and can decrease, in some circumstances, analytical uncertainty about smelting SI identifications. Such a procedure would have reduced the inclusion of some outlying SIs in the XP23 billet for instance. A pragmatic stance dictates inclusion of the *k*-means refinement step as a decision-making aid when group membership is questionable for some outlying SIs. Third, a procedure needs to be introduced for identifying cases where single iron objects are composite constructions smithed from metal produced at different sites or regions. One simple method, following that used by Dillmann and L'Héritier (2007), is to consider individually inclusions from different zones of interest within the artifact. Zones may be defined by weld lines or patterned differences in metallurgical phases.

8. Conclusions

Using the set of experimental smelting slag and SI compositional data generated by Blakelock et al. (2009), this paper has introduced and shown the utility of a comprehensive multivariate strategy for investigating the production origins of iron objects in the archaeological record. A model was introduced for defining SI types based on NRC compositional patterns. This offers several advantages over Dillmann and L'Héritier's (2007) linear regression approach. First, it examines multiple compounds simultaneously rather than by a series of pair-groups. Second, SI types are recognized by their relationship to patterns of variable correlation and can be removed in one stage rather than iteratively until an acceptable fit is achieved. Third, without the need for a fit requirement, there is greater certainty that most non-smelting SIs are identified. Finally, because SIs are grouped into functional types rather than labeled "normal" or "abnormal", it may be possible in future studies to investigate systematic variation in smithing styles between iron production workshops.

Fields created through multivariate ordination of −log transformed subcompositional ratios of smelting slag compounds and defined by KDEs were shown to be accurate representations of the chemical space occupied by smelting-derived SIs generated from the same ironmaking system. These fields are therefore an effective means of testing origin hypotheses of objects characterized by their average smelting-derived SI composition. PCA was successful when considering single and multiple group sourcing problems using experimental analogs. LDA was found to have an advantage over

PCA in separating training sets in multi-group provenance testing, though qualitative results were equivalent. All objects were correctly identified to the experiments that produced them in both PCA and LDA applications.

The strategy developed and tested in this paper is an attempt to adapt multivariate tools routinely used in ceramic provenance studies (e.g., Glascock, 1992; Neff et al., 2006) to the problem of sourcing iron artifacts. Focus is placed on exploiting the chemical signatures maintained between bloomery slag and artifact SIs to test provenance hypotheses. An alternative multivariate strategy emphasizing the chemical signatures maintained between ore and artifact SIs can be found in Leroy (2010) and Leroy et al. (2012). Multivariate techniques not only provide an efficient means of identifying and visualizing group structure in large compositional data sets, but also generate a chemical explanation for the observed patterns (Neff, 1994). These chemical explanations can be tested by reexamining the original data and can sometimes be observed by simpler plots of oxides and oxide-ratios. This study, therefore, extends the work of Blakelock et al. (2009) but does not replace the proven value of exploring patterns of oxides and oxide-ratios in iron provenance studies. An inspection of the loadings giving rise to Fig. 11, for example, suggest that nearly as much information could be gleaned from a direct comparison of MnO and TiO_2. PCA has generated a faster, though not different, result than a search through the space created by bivariate oxide comparisons. Situations that are more complex are possible, however, making some groups observable only through the application of multivariate methods. With regard to ceramic characterization, Glascock (1992, 16) notes that, "there is no single 'textbook' method for data reduction and interpretation that guarantees a satisfactory result for all applications. As a result, different approaches are required to achieve greater understanding of each data set." The present study offers a novel investigative framework to aid in testing origin hypotheses for iron objects that, in concert with other approaches, will contribute to a better understanding of the distribution and exchange of iron in the archaeological record.

Acknowledgments

Analyses of experimental slag and SIs discussed in this paper were undertaken at the UCL Wolfson Archaeological Science Laboratory and generously funded by the AHRC in the support of MSc research. We are grateful to the Amgueddfa Cymru, the National Museum of Wales, and all those involved in conducting the experimental ironmaking campaigns. Much gratitude is also owed to the staff and students at the UCL Institute of Archaeology for their expertise and support. Many of the ideas presented here evolved from discussions with Tom Birch and Bill Grimm. Comments and suggestions offered by Peter Crew and Sarah Paynter on an early draft of this paper led to several improvements. We also wish to thank an anonymous reviewer whose insightful remarks led us to clarify and extend several import points. Any errors reported in the text, however, remain the responsibility of the authors.

Appendix. Supplementary material

Supplementary data related to this article can be found online at doi:10.1016/j.jas.2012.02.037.

References

Aitchison, J., Barceló-Vidal, C., Pawlosky-Glahn, V., 2002. Some comments on compositional data analysis in archaeometry, in particular the fallacies in Tangri and Wright's dismissal of logratio analysis. Archaeometry 44, 295–304.

Baxter, M.J., 2001. Statistical modeling of artefact compositional data. Archaeometry 43, 131–147.

Baxter, M.J., 2006. A review of supervised and unsupervised pattern recognition in archaeometry. Archaeometry 48, 671–694.

Baxter, M.J., Beardah, C.C., Westwood, S., 2000. Sample size and related issues in the analysis of lead isotope data. Journal of Archaeological Science 27, 973–980.

Baxter, M.J., Beardah, C.C., Wright, R.V.S., 1997. Some archaeological applications of kernel density estimates. Journal of Archaeological Science 24, 347–354.

Baxter, M.J., Freestone, I.C., 2006. Log-ratio compositional data analysis in archaeometry. Archaeometry 48, 511–531.

Birch, T., Martinón-Torres, M., in press. The iron bars from the 'Gresham Ship': employing multivariate statistics to further slag inclusion analysis of ferrous objects, In: Bayley, J., Blakelock, E., Crossley, D. (Eds.), Iron and Ironworking: Proceedings of the archaeometallurgy conference, Bradford, November 2010. Historical Metallurgy Society, London.

Blakelock, E., Martinón-Torres, M., Veldhuijzen, H.A., Young, T., 2009. Slag inclusions in iron objects and the quest for provenance: an experiment and a case study. Journal of Archaeological Science 36, 1745–1757.

Buchwald, V.F., 2005. Iron and Steel in Ancient Times. The Royal Danish Academy of Sciences and Letters, Copenhagen.

Buchwald, V.F., Wivel, H., 1998. Slag analysis as a method for the characterization and provenancing of ancient iron objects. Materials Characterization 40, 73–96.

Charlton, M.F., 2009. Identifying iron production lineages: a case study in northwest Wales. In: Shennan, S.J. (Ed.), Pattern and Process in Cultural Evolution. University of California Press, Berkeley, pp. 133–144.

Charlton, M.F., Crew, P., Rehren, Th., Shennan, S.J., 2010. Explaining the evolution of ironmaking recipes—an example from northwest Wales. Journal of Anthropological Archaeology 29, 352–367.

Childs, W.R., 1981. England's iron trade in the fifteenth century. The Economic History Review 34, 25–47.

Cleere, H., 1975. The Roman iron industry of the Weald and its connexions with the *Classis Britannica*. Archaeological Journal 131, 171–199.

Cleere, H., 1986. Ironmaking in the economy of the ancient world: the potential of archaeometallurgy. In: Scott, B.G., Cleere, H. (Eds.), The Crafts of the Blacksmith. UISSP Comité pour la Sidérurgie Ancienne, Belfast, pp. 1–6.

Coustures, M.P., Béziat, D., Tollon, F., Domergue, C., Long, L., Rebiscoul, A., 2003. The use of trace element analysis of entrapped slag inclusions to establish ore – bar links: examples from two Gallo-Roman iron-making sites in France (Les Martys, Montagne Noire, and Les Ferrys, Loiret). Archaeometry 45, 599–613.

Coustures, M.P., Rico, C., Béziat, D., Djaoui, D., Long, L., Domergue, C., Tollon, F., 2006. La provence des barres de fer Romaines des Saintes-Maries-De-La-Mer (Bouches-Du_Rhône). Gallia 63, 243–261.

Crew, P., 1991. The experimental production of prehistoric bar iron. Historical Metallurgy 25, 21–36.

Crew, P., 1994. Currency bars in Great-Britain: typology and function. In: Mangin, M. (Ed.), La Sidérurgie Ancienne de l'Est de la France dans son Contexte Européen Actes du Colloque de Besançon, Paris, pp. 345–350.

Crew, P., 2000. The influence of clay and charcoal ash on bloomery slags. In: Tizzoni, C.C., Tizzoni, M. (Eds.), Iron in the Alps: Deposits, Mines and Metallurgy from Antiquity to the XVI Century, Bienno, pp. 38–48.

Degryse, P., Schneider, J.C., Kellens, N., Waelkens, M., Muchez, P., 2007. Tracing the resources of iron working at ancient Sagalassos (south-west Turkey): a combined lead and strontium isotope study on iron artifacts and ores. Archaeometry 49, 75–86.

Degryse, P., Schneider, J.C., Muchez, P., 2009. Combined Pb–Sr isotopic analysis in provenancing late Roman iron raw materials in the territory of Sagalassos (SW Turkey). Archaeological and Anthropological Sciences 1, 155–159.

Desaulty, A.-M., Mariet, C., Dillmann, P., Joron, J.L., Fluzin, P., 2008. The study of provenance of iron objects by ICP-MS multi-elemental analysis. Spectrochimica Acta Part B 63, 1253–1262.

Desaulty, A.-M., Dillmann, P., L'Héritier, M., Mariet, C., Gratuze, B., Joron, J.L., Fluzin, P., 2009. Does it come from Pays de Bray? Examination of an origin hypothesis for the ferrous reinforcements used in French medieval churches using major and trace element analyses. Journal of Archaeological Science 36, 2445–2462.

Devos, W., Senn-Luder, M., Moor, C., Salter, C., 2000. Laser ablation inductively coupled plasma mass spectrometry (LA-ICP-MS) for spatially resolved trace analysis of early-medieval archaeological iron finds. Journal of Analytical Chemistry 366, 873–880.

Dieudonné-Glad, N., 2000. L'atelier sidérurgique gallo-romain du Latté à Oulches (Indre). Gallia 57, 63–76.

Dillmann, P., L'Héritier, M., 2007. Slag inclusion analyses for studying ferrous alloys employed in French medieval buildings: supply of materials and diffusion of smelting processes. Journal of Archaeological Science 34, 1810–1823.

Fells, S., 1983. The Structure and Constitution of Ferrous Process Slags. Unpublished PhD thesis, University of Aston in Birmingham.

Glascock, M.D., 1992. Characterization of archaeological ceramics at MURR by neutron activation analysis and multivariate statistics. In: Neff, H. (Ed.), Chemical Characterization of Ceramic Pastes in Archaeology. Prehistory Press, Madison, pp. 11–26.

Gordon, R.B., 1997. Process deduced form ironmaking wastes and artefacts. Journal of Archaeological Science 24, 9–18.

Gordon, R.B., van der Merwe, N.J., 1984. Metallographic study of iron artefacts from the eastern Transvaal, South Africa. Archaeometry 26, 108–127.

Hamilton, H.C., Falconer, W. (Translators), 1903. The Geography of Strabo. George Bell & Sons, London.

Hedges, R.E.M., Salter, C.J., 1979. Source determination of iron currency bars through analysis of the slag inclusions. Archaeometry 22, 161–175.

Jones, M.C., Marron, J.S., Sheather, S.J., 1996. A brief survey of bandwidth selection for density estimation. Journal of the American Statistical Association 91, 401–407.
Krzanowski, W.J., 2000. Principles of Multivariate Analysis: A User's Perspective, Revised Edition. Oxford University Press, Oxford.
Leroy, S., 2010. Circulation au Moyen Äge des matériaux ferreux issus des Pyrénées ariégeoises et de la Lombardie. Apport du couplage des analyses en éléments traces et multivariées, Unpublished PhD thesis, Université Technologique de Belfort-Montbéliard.
Leroy, S., Cohen, S.X., Verna, C., Gratuze, B., Téreygeol, Fluzin, P., Bertrand, L., Dillmann, P., 2012. The medieval iron market in Ariège (France). Multidisciplinary analytical approach and multivariate analyses. Journal of Archaeological Science 39, 1080–1093.
Leroy, S., Simon, R., Bertrand, L., Williams, A., Foy, E., Dillman, P., 2011. First examination of slag inclusions in medieval armours by confocal SR-μ-XRF and LA-ICP-MS. Journal of Analytical Atomic Spectrometry 26, 1078–1087.
Morton, G.R., Wingrove, J., 1972. Constitution of bloomery slags: part II: medieval. Journal of the Iron and Steel Institute 210, 478–488.
Neff, H., 1994. RQ-mode principal components analysis of ceramic compositional data. Archaeometry 36, 115–130.
Neff, H., 2000. Neutron activation analysis for provenance determination in archaeology. In: Ciliberto, E., Spoto, G. (Eds.), Modern Analytical Methods in Art and Archaeology. John Wiley and Sons, New York, pp. 81–134.
Neff, H., Blomster, J., Glascock, M.D., Bishop, R.L., Blackman, M.J., Coe, M.D., Cowgill, G.L., Diehl, R.A., Houston, S., Joyce, A.A., Lipo, C.P., Stark, B.L., Winter, M., 2006. Methodological issues in the provenance investigation of Early Formative Mesoamerican ceramics. Latin American Antiquity 17, 54–76.
Paynter, S., 2006. Regional variations in bloomery smelting slag of the Iron Age and Romano-British periods. Archaeometry 48, 271–292.
R Development Core Team, 2010. R: A Language and Environment for Statistical Computing. R Foundation for Statistical Computing, Vienna. URL: http://www.R-project.org.
Rostoker, W., Bronson, B., 1990. Pre-industrial Iron: Its Technology and Ethnology. (Archeomaterials Monograph 1). Philadelphia.
Rostoker, W., Dvorak, J.R., 1990. Wrought irons: distinguishing between processes. Archeomaterials 4, 153–166.
Salzman, L.F., 1952. Building in England Down to 1540: A Documentary History. Oxford University Press, Oxford.
Sayre, E.V., 1975. Brookhaven procedures for statistical analyses of multivariate archaeometric data, Unpublished Report BNL-23128, Brookhaven National Laboratory, Upton.
Schwab, R., Heger, D., Höppner, B., Pernicka, E., 2006. The provenance of iron artefacts from Manching: a multi-technique approach. Archaeometry 48, 433–452.
Sheather, S.J., 2004. Density estimation. Statistical Science 19, 588–597.
Sheather, S.J., Jones, M.C., 1991. A reliable data-based bandwidth selection method for kernel density estimation. Journal of the Royal Statistical Society, Series B 53, 683–690.
Smith, K.E.S., 1995. Iron-working in north-west Wales in the late fourteenth century. Archaeological Journal 152, 246–290.
Starley, D., 1999. Determining the technological origins of iron and steel. Journal of Archaeological Science 26, 1127–1133.
Tangri, D., Wright, R.V.S., 1993. Multivariate analysis of compositional data: applied comparisons favour standard principal components analysis over Aitchison's loglinear contrast method. Archaeometry 35, 103–112.
Threlfall-Holmes, M., 1999. Late medieval iron production and trade in the north-East. Archaeologia Aeliana 27, 109–122.
Veldhuijzen, H.A., Rehren, Th, 2007. Slags and the city: early iron production at Tell Hammeh, Jordan, and Tel Beth-Shemesh, Israel. In: La Niece, S., Hook, D., Craddock, P. (Eds.), Metals and Mines: Studies in Archaeometallurgy. Archetype Publications, London, pp. 189–201.
Venables, W.N., Ripley, B.D., 2002. Modern Applied Statistics with S, fourth ed. Springer, New York.